Solute Segregation and Hydrogen-Induced Intergranular Fracture in an Alloy Steel

JUN KAMEDA and C. J. McMAHON, Jr.

Hydrogen-induced intergranular fracture of laboratory heats of a 3.5 Ni-1.7 Cr steel doped with P, Sn, or Sb and having a yield strength of 840 MPa and a prior austenite grain size of 120 μm has been compared with that of an undoped steel at a hydrogen pressure of 0.17 MPa (1.68 atm). The intergranular concentrations of the impurities were controlled by varying the time of aging at 480 °C. Cracking of the undoped steel tested in hydrogen occurred along martensitic lath boundaries at high stresses. However, the susceptibility of the doped steels to hydrogen-induced intergranular cracking increased precipitously with impurity concentration. The susceptibility was measured in terms of the threshold stress intensity K_{th} for the first detectable crack extension in precracked specimens and in terms of the threshold stress σ_{th} for microcrack formation in notched specimens. A comparison between the intergranular strength in hydrogen and in air revealed that absorption of hydrogen produced a profound intergranular weakening when the grain boundaries contained even a small amount of a segregated embrittling element. The relative embrittling potencies of P, Sn, and Sb in hydrogen gas were the same as in air. The combined effects of hydrogen and the impurities in reducing intergranular cohesion are discussed in terms of a newly proposed dynamic model which takes into account the accumulation of hydrogen ahead of a moving microcrack.

I. INTRODUCTION

IT is generally recognized that hydrogen-induced cracking in medium-to-high strength ferritic steels occurs along prior austenitic grain boundaries.[1-8] For example, it has been found[9] for 4340 steels that the threshold stress intensity K_{th} for hydrogen-induced cracking is inversely related to the percentage of intergranular fracture. It has been demonstrated[9,10,11] for several types of alloy steel tested in relatively low-fugacity hydrogen that the intergranular cracking tendency increases with the intergranular concentration of known embrittling elements, such as P, Sn, *etc*. In the case of HY 130 steel it was recently found[12] that, if the segregated impurity level becomes low enough, the cracking mode in hydrogen switches from stress-controlled intergranular fracture to a displacement-controlled mode which does not involve prior austenite grain boundaries. Since the latter mode occurred at high apparent stress intensities and resulted in crack-tip bifurcation, it cannot be considered as brittle behavior in the same sense as the intergranular cracking.

It is clear that the improvement of the toughness of such steels in hydrogen, or hydrogen-producing environments, will require the inhibition of intergranular cracking. The work reported on here was undertaken to provide a better understanding of the mechanisms of intergranular cracking in hydrogen and the factors which control it. For this purpose we used the 3.5 pct Ni-1.7 pct Cr steel, doped with either P, Sn, or Sb, previously employed[13,14] in the studies of the effects of these impurities on intergranular strength. The hydrogen-induced cracking behavior was characterized in terms of K_{th} in precracked specimens and the local tensile stress for microcrack nucleation in notched specimens, both of which were stressed in hydrogen gas at just above atmospheric pressure.

JUN KAMEDA, formerly with the Department of Materials Science and Engineering, University of Pennsylvania, is now Associate Metallurgist with Metals Development, Ames Laboratory, Iowa State University, Ames, IA 50011. C. J. McMAHON, Jr. is Professor, Department of Materials Science and Engineering, University of Pennsylvania, Philadelphia, PA 19104.

Manuscript submitted November 9, 1981.

II. EXPERIMENTAL PROCEDURE

This study employed vacuum-melted laboratory heats of Ni-Cr steel; one heat was undoped and the others were individually doped with Sb, Sn, or P; the compositions are listed in Table I. The steels were austenitized at 1025 °C for one hour and oil-quenched, then tempered at 600 °C for one hour; the average prior austenite grain size was 120 μm and the hardness was Rc 30. The 0.02 pct offset yield strength was 840 MPa (120 ksi). Doped specimens were aged at 480 °C for different times to allow various amounts of intergranular solute segregation. Precracked compact tension specimens of 1 inch (25.4 mm) crack length and 0.5 inch (12.7 mm) thickness with 0.05 inch (1.27 mm) deep side grooves, and notched four-point specimens of the type used previously[13,14] were tested in air and in hydrogen, and the results were compared with those of previous tests in air. The hydrogen tests were performed at 23 ±2 °C in a stainless steel chamber which had been evacuated to $<1 \times 10^{-5}$ torr (<1.3 MPa) and then refilled to 0.17 MPa (1.68 atm) of high purity hydrogen (commercial grade 5) that had been passed through a palladium purifier and a liquid nitrogen cold trap. After the hydrogen was introduced, the specimens were loaded using a cross-head speed

Table I. Chemical Compositions of Steels (Wt Pct)

Steel	Ni	Cr	C	P	S	Sb	Sn
Undoped	3.5	1.7	0.3	0.004	0.004	—	—
Sb-doped	3.5	1.7	0.29	0.004	0.004	0.056	—
Sn-doped	3.5	1.7	0.29	0.004	0.004	—	0.061
P-doped I	3.5	1.7	0.3	0.060	—	—	—
P-doped II	3.5	1.7	0.3	0.040	—	—	—

of 5.1 × 10^{-3}mm per minute in a screw-driven testing machine. For the precracked specimens the curves of load *vs* clip gauge displacement (CGD) at the mouth of the precrack were measured. The values of K_{th} were computed from the load which corresponded to the first discontinuity in the load *vs* CGD curve. Precracking was applied to all of the compact tension specimens and to one of the notched bars in accordance with the ASTM specification,[15] the ΔK range was 10 to 30 MPa$\sqrt{m}$, depending on the values of K_{th} of the various specimens.

Four-point bend tests were performed on the same steels under the same conditions. The finite element elastic-plastic stress analysis of Griffiths and Owen[16] was used to calculate the stress distribution ahead of the notch as a function of load. Measurements of acoustic emission (AE) and interrupted-loading experiments were performed in order to examine the microscopic details of the early stages of hydrogen-induced intergranular cracking on one precracked specimen and on several notched specimens. The interrupted-test notched bend samples were deembrittled at 670 °C for 30 minutes and then cracked further at room temperature by fatigue; the fracture surfaces were examined using scanning electron microscopy (SEM). The results of selected-area Auger electron spectroscopy (AES) on the same steels from the previous studies[13,14] were utilized.

III. RESULTS

Precracked specimens of the undoped steel which had been aged for 1000 hours at 480 °C and the Sb-doped steel which had been aged for 40 hours at 480 °C were tested in 0.17 MPa hydrogen at 23 °C. (The undoped steel showed very little susceptibility to temper embrittlement and exhibited no intergranular fracture when tested in air at room temperature after a 1000-hour aging period.) The load *vs* clip gauge displacement (CGD) curves for the hydrogen tests are shown in Figure 1. For the undoped sample we see a gradual departure from linearity. The apparent K_{th} value determined from the load corresponding to the deviation from linearity was greater than 120 MPa$\sqrt{m}$. The Sb-doped specimen exhibited a "pop-in" at a low load followed by bursts of cracking and then rapid fracture. The K_{th} value was

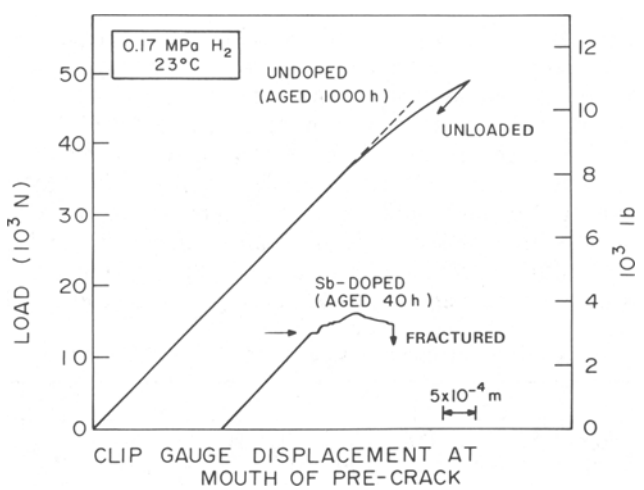

Fig. 1 — Comparison between load *vs* clip gauge displacement for precracked specimen of undoped steel (aged 1000 h) and for Sb-doped steel (aged 40 h).

30 MPa$\sqrt{m}$, as determined from the pop-in load. Examination of the undoped specimen after it was unloaded and fractured in air showed that the initial crack extension occurred as a bifurcation of the precrack by mode II shear cracking. This bifurcation can be seen in Figure 2. A midplane section showing the lower branch of the bifurcated precrack tip is shown in Figure 3. The region of hydrogen-induced crack growth in the undoped specimen was examined by scanning electron microscopy. It was found that the

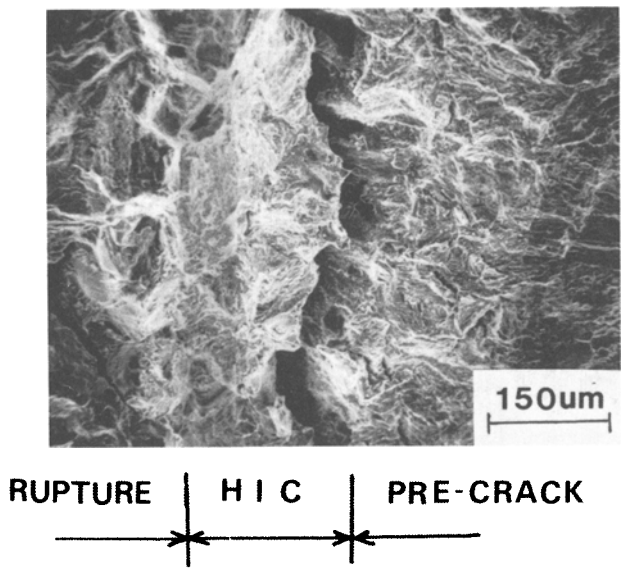

Fig. 2 — Scanning electron micrograph of unaged steel loaded in H_2 and then fractured (by rupture) in air, showing extent of hydrogen-induced cracking (HIC).

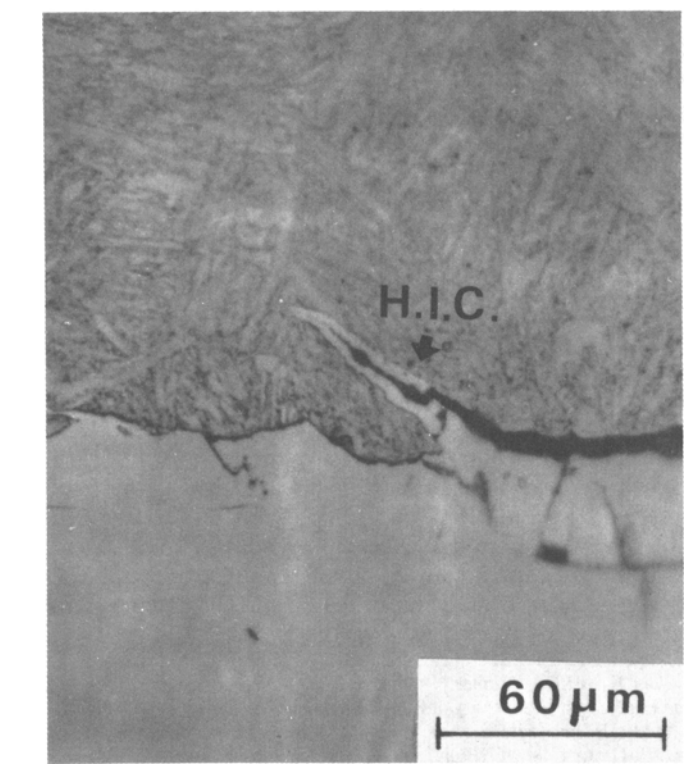

Fig. 3 — Midplane section of precracked specimen of undoped steel loaded in H_2 gas, showing bifurcation at tip of precrack.

fracture did not occur along prior austenite grain boundaries, but rather along what appeared to be boundaries of laths or lath colonies in the tempered martensite microstructure, as shown in Figure 4. Similar observations of crack tip bifurcation in unembrittled specimens and a similar fracture mode have been observed previously in a 5 pct Ni steel.[12]

In contrast to the behavior of the undoped steel, the fracture mode in the Sb-doped specimens tested in hydrogen was nearly 100 pct intergranular; this is similar to what is generally observed in commercial steels subjected to hydrogen-induced cracking. In order to examine the hydrogen-induced cracking behavior of the Sb-doped steel in more detail, acoustic emissions were recorded during the tests. Table II shows that in a sample aged for 10 hours, high energy acoustic emissions began at K levels greater than 20 MPa$\sqrt{m}$, but well below the K level corresponding to the pop-in event (indicated by an arrow). These signals increased in number and energy as the pop-in level was approached. A similar sample was loaded up to the point of the first few high energy acoustic emissions, then unloaded, removed from the test chamber, and carefully fatigue cracked in air using a low ΔK and K_{max} (~7 MPa$\sqrt{m}$) to suppress any tendency for further intergranular cracking during the fatigue. The sample was then broken open and examined in the SEM. Figure 5(a) shows one of several patches of intergranular fracture found just ahead of the tip of the precrack. This intergranular cracking, which was not detected by the load *vs* CGD measurements, presumably gave rise to the acoustic emissions. (The same kind of observation was made in specimens tested in air.[17]) Another similar specimen was unloaded just after the pop-in event and then fatigued in air in the same manner. Figure 5(b) shows a typical example of one patch of intergranular fracture ahead of the precrack; the intergranular patches had become considerably larger than when first detectable by AE.

These experiments show that the K_{th} value determined from the pop-in load is a function of the sensitivity of the load *vs* CGD measurements. This K_{th} is simply a manifestation of the occurrence of some minimally detectable extent of intergranular cracking at discrete locations along the tip of the precrack. Clearly, the intergranular hydrogen-induced crack extension does not occur uniformly across the

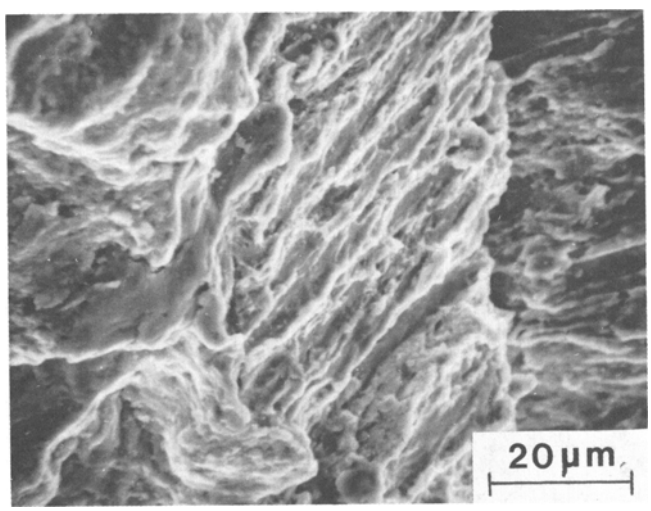

Fig. 4—Interlath fracture in tempered martensite in the undoped steel.

Table II. AE Event Count on Sb-Doped Steel Aged for 10 Hours (AE Gain: 40 dB, Frequency Range: 100 KHz to 1 MHz)

Tested in H_2	$K_{MPa\sqrt{m}}$							
E_{AE} (Arb. Units)	19 to 21	21 to 23	23 to 25	25 to 27	27 to 29	29 to 31	31 to 33 ▼	33 to 35
0.2	—	1	—	—	—	—	3	3
0.5	—	—	—	—	—	—	—	—
0.75	—	1	—	—	—	1	—	—
1.0	—	—	—	1	—	—	1	—
1.5	—	—	—	—	1	—	1	—
1.75	—	2	1	1	—	2	2	—
2.0	—	—	—	1	3	5	1	6
2.5	—	—	—	—	—	—	—	—

Noise level ≤0.1
K_{th} = 33 MPa$\sqrt{m}$

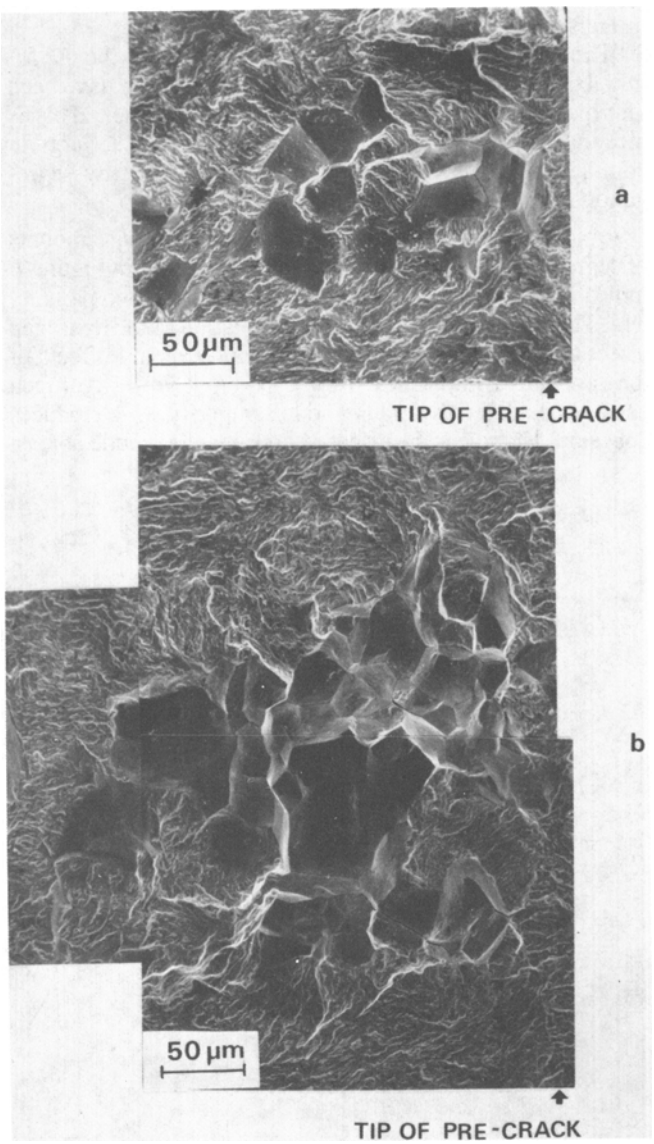

Fig. 5—Hydrogen-induced intergranular cracking adjacent to precrack tip in Sb-doped steel aged 10 h. Specimens were unloaded and fatigued in air after loading to (*a*) 75 pct of "pop-in" load and (*b*) just after "pop-in" load.

front of the precrack, and the beginning is not detectable by the usual techniques of load *vs* CGD measurements.

It has been pointed out[17] that the same detection problem occurs in tests of embrittled specimens in air. Intergranular cracking can be detected by AE well below K_{Ic} as determined by the pop-in load. Thus, in both air and hydrogen tests the K_{Ic} or K_{th} values are characteristic not of the strength of the weakest grain boundary, but of some average intergranular strength, as determined by the amount and distribution of impurity segregation.

By variation of the time of aging at 480 °C the extent of intergranular segregation was varied in the steels doped with Sb, Sn, and P, as in the previous work,[13,14] and the effects on K_{Ic} in air[17] and K_{th} in hydrogen were compared as shown in Figure 6. These results indicate the following:

1. The effects of the impurities on the values of K_{th} in hydrogen are similar to those on K_{Ic} in air.
2. As the K level for cracking decreases, the K_{th} and K_{Ic} values tend to converge; *i.e.*, the effect of hydrogen diminishes.
3. The largest hydrogen-induced reduction in the K for initial crack extension is found in the steels which have been only partially embrittled by any of the impurities. This is presumably why the effects of hydrogen can be so large in commercial steels in which the effects of impurity segregation are often undetectable by fracture tests in air.

A plot of K_{th} in hydrogen *vs* K_{Ic} in air for various amounts of segregation of the three impurities, as shown in Figure 7, indicates a fairly close correlation between the two parameters. This is consistent with an interpretation of the hydrogen effect as being simply additive to the preexisting effects of the segregated impurities. In this point of view, hydrogen can be considered as simply another impurity which reduces cohesion. However, the effect of hydrogen is unique at least because of its high mobility in the crystal lattice of the steel; this enables the hydrogen to migrate rapidly at room temperature and become concentrated at regions of high tensile stress (due to the large lattice expansion associated with hydrogen dissolved in iron).

Data such as shown in Figure 6 are useful for engineering purposes, since they characterize the resistance of a steel to the growth of preexisting cracks. However, such data can not be interpreted in a microscopic manner for two reasons. First, there is the problem regarding the dependence of K_{th} on the sensitivity of measurement, as discussed above. The second problem has to do with the very restricted volume of highly-stressed material ahead of the tip of a precrack and the fact that the microscopic processes of decohesion which occur there are affected more by the stress gradient in that region than by the value of the maximum stress. These issues have been discussed elsewhere.[17]

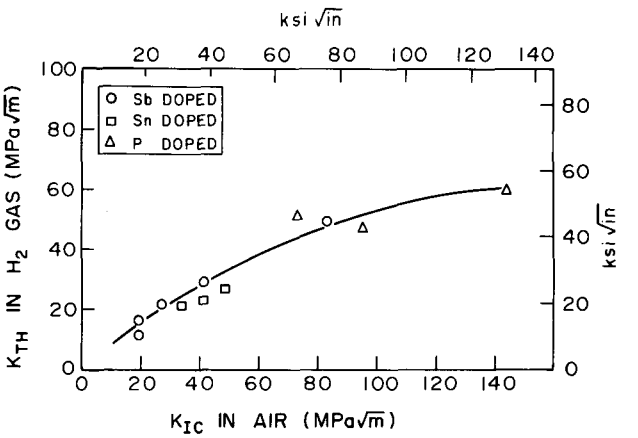

Fig. 7—Correlation between K_{th} in H_2 and K_{Ic} in air in steels with several impurities aged for various times.

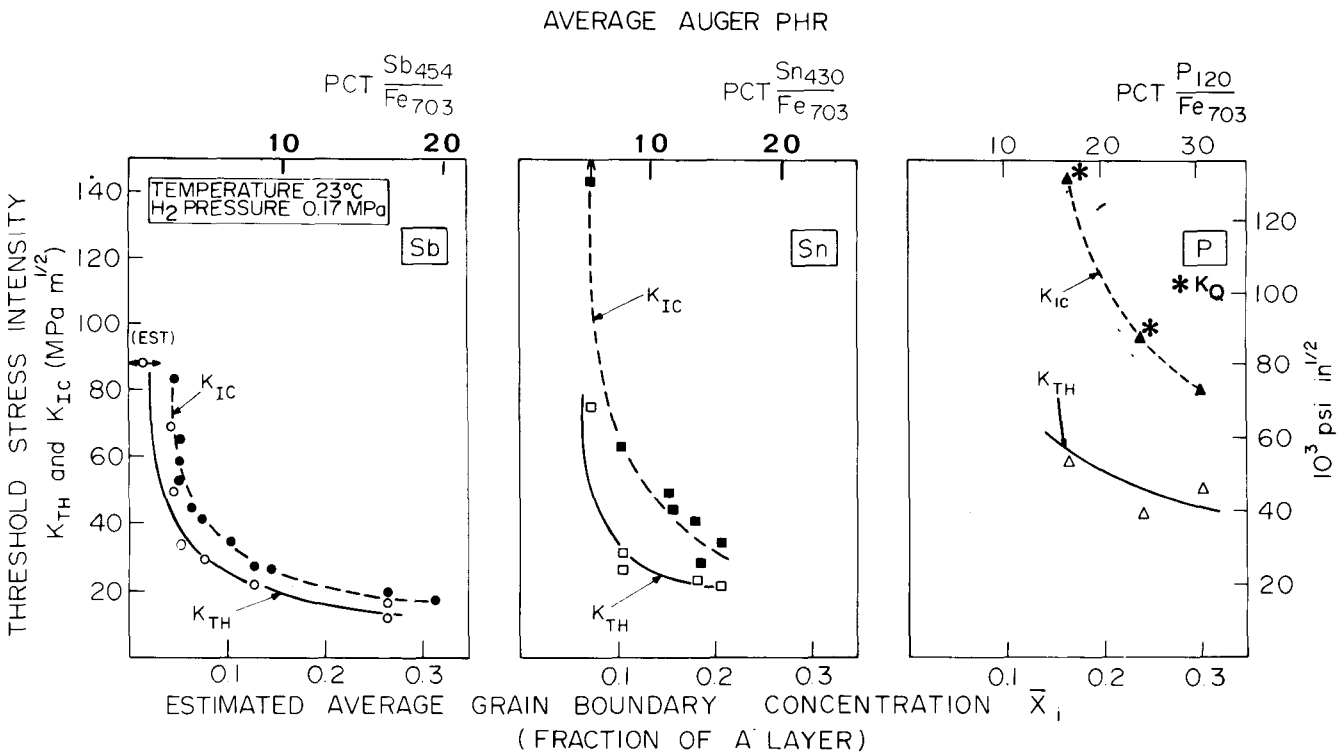

Fig. 6—Variations of K_{th} and K_{Ic} with average intergranular concentration $\bar{X}_i$ of Sb, Sn, or P. (This figure was quoted in Ref. 25.)

These problems can be largely eliminated by the use of notched specimens in which the volume of highly-stressed material is relatively large, the stress gradient in that volume is relatively small, and the maximum stress in that volume varies significantly with the applied load. Examples of the load-displacement curves for the Sb-doped notched specimens tested in pure bending are given in Figure 8. In all cases the fractures were nearly 100 pct intergranular. Acoustic emission measurements were made on the samples aged for 40 hours and tested in air and in hydrogen. The data are given in Table III, and they show no significant difference between the air and the hydrogen tests. In each sample the high energy acoustic emissions (see circled data) started just above a maximum local stress of 1200 MPa, which is only 60 pct of the fracture value in air, previously[13] designated as σ^*.

The sources of the acoustic emissions in the specimen tested in air could not be determined by the SEM observations of unloaded and post-test-fatigued specimens. Figure 9 shows a typical portion of the post-test-fatigue fracture surface of a specimen which was stressed to 98 pct of maximum load (in air), then unloaded, deembrittled, and fatigue cracked. No sign of any intergranular cracking could be found. This supports the position taken earlier[13,14] that the first intergranular microcrack forms at σ^* and leads directly to total failure of the specimen. We assume that the high energy AE signals at the lower stresses were due to the brittle cracking of nonmetallic inclusions at stresses too low

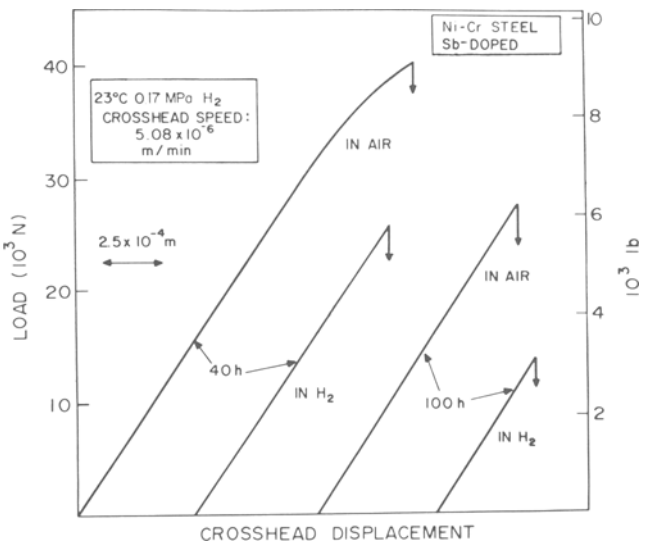

Fig. 8—Examples of load *vs* deflection curves for notched bar specimens tested in air and H_2 gas.

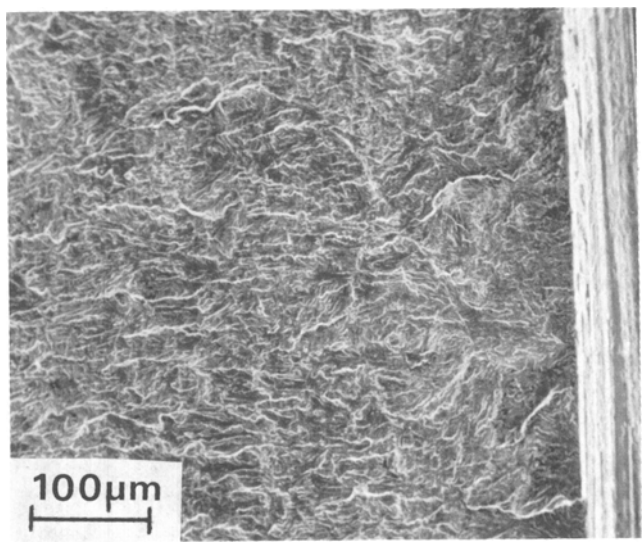

Fig. 9—Scanning electron micrograph of Sb-doped steel which was unloaded at 98 pct of load corresponding to σ^* and fatigued in air. No indication of intergranular microcracking could be found.

Table III. AE Event Count on Sb-Doped Steel Aged for 40 Hours (AE Gain: 40 dB, Frequency Range: 100 KH_z to 1 MH_z)

Tested in Air	σ_L (MPa)											
E_{AE} (Arb. Units)	900 to 1000	1000 to 1100	1100 to 1200	1200 to 1300	1300 to 1400	1400 to 1500	1500 to 1600	1600 to 1700	1700 to 1800	1800 to 1900	1900 to 2000	2000 to 2050 σ^*
0.3	—	1	—	—	1	1	—	—	2	2	—	—
0.5	—	1	—	—	—	—	—	—	—	—	—	—
0.75	—	0	—	1	—	—	—	—	—	—	—	—
1.0	2	2	—	—	—	—	—	—	—	—	—	—
1.5	—	—	—	—	—	1	—	—	—	—	—	—
1.75	—	—	—	(1)	—	4	1	—	—	3	3	1
2.0	—	—	—	—	—	—	2	1	—	3	2	2

Tested in H_2	σ_L (MPa)								
E_{AE} (Arb. Units)	900 to 1000	1000 to 1100	1100 to 1200	1200 to 1300	1300 to 1400	1400 to 1500	1500 to 1600	1600 to 1700	1700 to 1750
						σ_{th}			
0.3	—	—	—	1	—	2	—	—	—
0.5	—	—	—	1	—	—	—	—	—
0.75	—	—	—	—	—	—	—	1	1
1.0	—	—	—	—	—	—	—	—	—
1.5	1	—	—	—	—	—	—	—	—
1.75	—	—	—	1	2	—	2	—	—
2.0	—	—	—	(1)	1	4	1	7	2

for propagation to occur across a whole intergranular facet.

Similar interrupted tests were carried out in hydrogen, and these showed that facet-size intergranular microcracks did form at stresses below the maximum local stress at which fracture occurred in hydrogen. (We designate the latter as σ_H^*.) Tests in hydrogen were interrupted at progressively lower loads, and the specimens were deembrittled and fatigue-cracked and examined in the SEM. The maximum load was reduced until no intergranular microcracks could be found. The lowest stress at which the facet-size intergranular microcracks were found we designate as σ_{th}, the threshold value of the maximum local tensile stress for hydrogen-induced microcracking. Figure 10 shows one of two patches of intergranular microcracking which could be found in the Sb-doped specimen aged for 40 hours and unloaded just after σ_{th} was reached. In all such cases the first intergranular microcracks were found ahead of the tip of the notch; that is, they were never connected with the free surface. This means that hydrogen traveled through the steel, by either diffusion or dislocation transport or both, to the region where the intergranular microcracking began. We take this as conclusive evidence that hydrogen causes intergranular brittle fracture in steel by collecting at regions of high tensile stress and by further lowering of the cohesive strength along grain boundaries already weakened by segregated impurities.

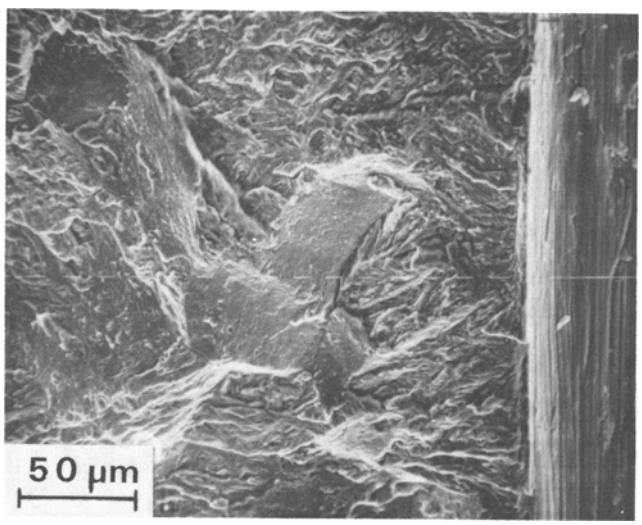

Fig. 10—Scanning electron micrograph of Sb-doped steel which was loaded in H_2 just to σ_{th}, then unloaded and fatigued in air. One of 2 isolated facet-size intergranular microcracks ahead of notch is shown.

From the AE measurements it was apparent that the formation of intergranular microcracks such as shown in Figure 10 could not be distinguished from whatever events produced the AE in the specimens tested in air. Since the AE method could not be used to detect the first hydrogen-induced facet-size intergranular microcracks, it was necessary to do interrupted tests followed by deembrittlement, fatigue cracking, and subsequent SEM observations on specimens aged for different times in order to establish the dependence of σ_{th} on the amount and kind of segregated impurity. By means of this very laborious process the results shown in Figure 11 were obtained.

In some respects these results are similar to those found for the precracked specimens (Figure 6). The largest effects of hydrogen are found at the lower levels of impurity segregation; σ_{th} drops precipitously in the early stages of impurity segregation. In the Sb-doped specimens σ_{th} converges with σ^* at large amounts of Sb segregation. This means that the hydrogen in the heavily embrittled steel had no apparent effect on intergranular embrittlement. A comparison between the values of σ_{th} and σ^* indicates that the presence of hydrogen absorbed by a partially embrittled steel produced substantial reductions in cohesive strength.

The curves labeled σ_H^* in Figure 11 represent unstable fracture in the specimens tested in hydrogen. In the stress range between σ_{th} and σ_H^* intergranular microcracks continued to form discretely until the stress high enough for unstable propagation (*i.e.*, σ_H^*) was reached. In the air tests the stress for the formation of facet-size intergranular microcrack was apparently equal to or greater than that needed for unstable propagation. Thus, it appears that fracture in air is controlled by the formation of an intergranular microcrack

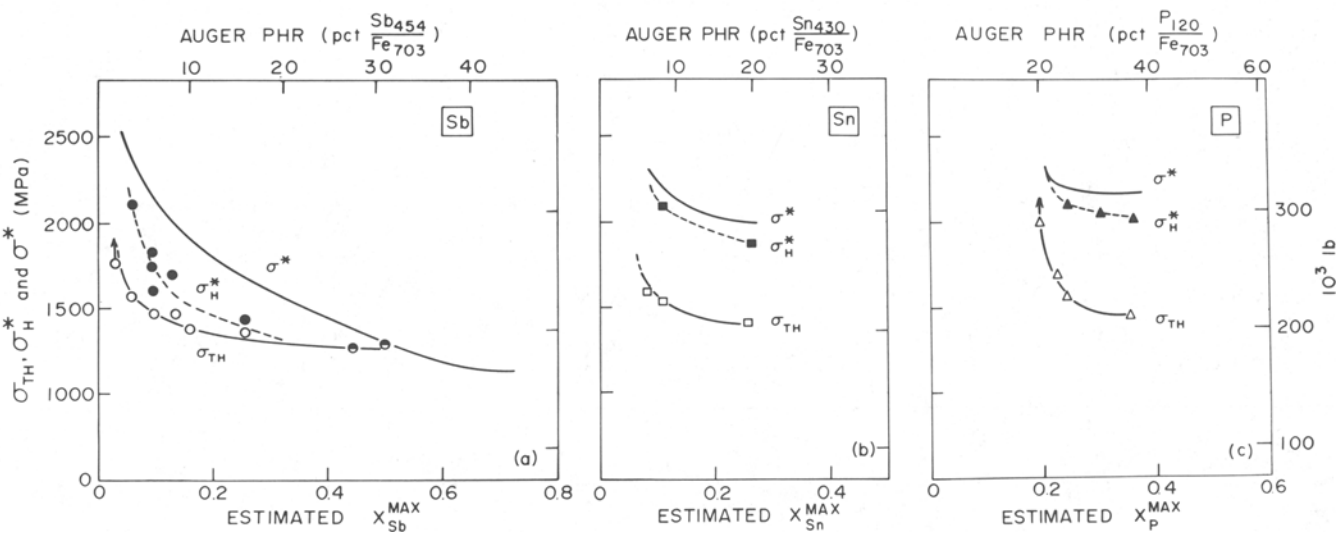

Fig. 11—Variations of intergranular strength σ_{th} and σ_H^* with grain boundary concentration of several solute impurities. Also plotted are the curves for σ^* in air.

(except at the highest Sb concentrations). It appears that the effect of hydrogen is mainly to reduce the critical stress necessary for the formation of a facet-size microcrack below that needed for long range propagation.

IV. DISCUSSION

It has been reported previously[13,14] that the local stress σ^* necessary to initiate intergranular brittle fracture in a quenched and tempered alloy steel decreases as the concentration of segregated metalloid impurities increases. This has been interpreted as resulting from a reduction in cohesive strength in proportion to the impurity concentration. It has been rationalized semi-quantitatively in terms of a model[18,19] which accounts for the relationship between the ideal work of fracture, W_i, (or the cohesive energy) and the plastic work, W_p, dissipated during the extension of a brittle crack because of dislocation emission from the crack tip.

The present research shows that when such steels are tested in low pressure hydrogen gas, hydrogen is transported to regions of high tensile stress, and this can result in the formation of intergranular microcracks at low stress levels. This cracking is a combined effect of the previously segregated impurity and the hydrogen absorbed during the test. If the intergranular impurity concentration is too low, intergranular brittle fracture (*i.e.*, along prior austenite grain boundaries) does not occur at this hydrogen pressure. Instead, another type of decohesion occurs along martensitic lath boundaries at high stress levels. The embrittling effect of hydrogen is greatest at low to intermediate levels of impurity segregation; in a steel severely embrittled by impurity segregation the effect of hydrogen can be negligible.

When a notched specimen is loaded in pure bending in hydrogen, intergranular microcracks begin to form once a threshold value of the maximum local stress, σ_{th}, is reached. Such microcracks continue to form in a discontinuous manner until the stress for long range propagation σ_H^* is reached. This local stress, σ_H^*, is found to be lower than the microcrack nucleation stress in air, σ^*. Thus, except for the most severely embrittled steels, intergranular brittle failure in air is controlled by the formation of a facet-size microcrack, whereas in hydrogen the nucleation stress, σ_{th}, is generally below the long-range propagation stress.

In a precracked Sb-doped specimen aged for 10 hours and loaded in hydrogen, the first intergranular cracking was detected by AE at a stress intensity of less than 23 MPa$\sqrt{m}$ (see Table II), whereas when an identical specimen was loaded in air,[17] the first intergranular cracking was detected by AE at a stress intensity of greater than 30 MPa$\sqrt{m}$. Thus, the effect of hydrogen in the precracked specimen is similar to that in the notched specimen.

The present results give strong support to the "decohesion model" of hydrogen embrittlement. It is clear that in the notched samples the formation of brittle cracks occurs internally as a result of absorption of hydrogen by the steel, transport of this hydrogen to weak grain boundaries in regions of high tensile stress ahead of the notch, and hydrogen-induced reduction in cohesion at those boundaries. The fact that the initial hydrogen-induced microcracks in the notched specimens formed in the region ahead of the notch in the region of the maximum principal stress (and maximum hydrostatic tension) is consistent with the model due originally to Troiano and co-workers[20,21] and later elaborated by Oriani *et al*[3,22] which treats the effect of dissolved hydrogen in terms of the equilibrium concentration of hydrogen in the highly-stressed material ahead of a precrack or notch.

Knowing the hydrostatic tension, the temperature, the atomic volume of hydrogen in iron, and the hydrogen solubility in the absence of stress, the equilibrium hydrogen concentration in the region of maximum tension can be calculated from thermodynamics.[23] However, it has been shown recently[24] that when appropriate values of the physical constants are used, this hydrogen concentration in the present notched specimens would be only of the order of 10^{-6} (atom fraction), a value that must be too low by several orders of magnitude to explain the observed effects on intergranular cohesion.

In order to account for the kind of enhancement of the local hydrogen concentration which must occur to produce the observed effects, Kameda and Jokl[24] have proposed that hydrogen is trapped in the stress field of a microcrack tip as it extends from the nucleus and that this hydrogen is carried along with the crack tip so that the hydrogen concentration there continuously increases. This accumulation would occur as hydrogen is carried along with the microcrack tip, as illustrated schematically in Figure 12. Hydrogen atoms in lattice sites just adjacent to the crack plane are pushed forward by a kind of pumping mechanism as the expanded lattice collapses back to its normal dimensions behind each row of broken bonds. In this way sites labeled 1 in Figure 12 are filled. This process is not comparable to normal lattice diffusion, since the hydrogen atom jumps are driven by very large local energy gradients and must therefore be highly directional. Thus, the hydrogen can move at rates much higher than normal lattice diffusion and thereby keep up with the microcrack as it accelerates. In addition, hydrogen atoms lying on the crack plane should be pulled forward to site-type 2 as bonds break, because the chemical potential of hydrogen is lower in the expanded lattice at the crack tip than it would be if the hydrogen were left behind adsorbed on the fracture surface.

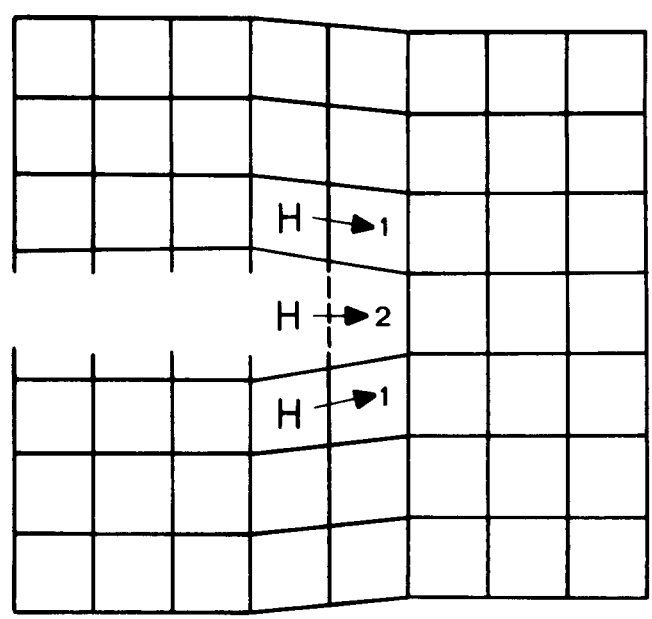

Fig. 12—Hydrogen atom movements envisioned to occur at the tip of a moving microcrack.

As the microcrack velocity increases, the rate of increase of the crack tip hydrogen concentration presumably slows down due to the eventual failure of all of the hydrogen to keep up with the accelerating microcrack tip. Also, as the brittle crack becomes large the elastic energy release rate would become so large that the value of W_i would become unimportant. Thus, the hydrogen effect should be most important in the initiation of brittle fracture, that is, in the creation of intergranular microcracks several facets in extent (on the order of a few hundred μm).

This dynamic model of hydrogen-induced cracking[24] connects with the previously-discussed[13,14,17–19] model of brittle fracture initiation in steels in the following way: In order for an intergranular microcrack of one-or-more grain diameters in size to be formed in the stress field of a notch or precrack, it must accelerate, rather than decelerate, as it leaves the inclusion which serves as its nucleus. Hence, in a steel with some given maximum segregation level (*i.e.*, minimum intergranular strength), some threshold stress σ^* is necessary for the formation of a microcrack in the absence of hydrogen. If hydrogen in or near the grain boundary can be captured by the tip of a nascent microcrack as it spreads from its nucleus in a specimen loaded to a maximum stress below σ^*, a decelerating microcrack can reaccelerate, since the increasing hydrogen concentration in the crack tip region effectively produces a continuously decreasing intergranular strength. Thus, in this model the effects of the hydrogen and the already-segregated intergranular impurities would be additive, and the microcrack nucleation stress, which we have called σ_{th}, would lie below σ^*.

We should emphasize that this is a microscopic model which deals with microcrack formation. Unstable cracking in hydrogen in a notched bar (at σ_H^*) or in a precracked sample (at $>K_{th}$) is presumably not so much affected by the hydrogen because of the high crack velocities involved. That is why we believe that σ_H^* would approximate the local stress for crack propagation in a notched bar in air.

In steels having insufficient impurity segregation to allow the growth of a microcrack to a size of one or more facets, the brittle intergranular cracking mode is not found in the present low-pressure hydrogen atmosphere. Instead, cracking along lath boundaries of the tempered martensite occurs in a quasi-static fashion. Although the cracking along lath boundaries is probably more complicated than brittle cracking along prior austentite grain boundaries, we suggest that the role of dislocations in transporting and building up hydrogen at lath boundaries becomes important. As emphasized previously,[12] this is a relatively benign form of hydrogen-induced cracking, because it occurs at high stresses and is essentially displacement-controlled.

Finally, it must be pointed out that the behavior of the σ_{th} curve for the Sb-doped steel (Figure 11) at high intergranular Sb concentrations is unexpected and will need further investigation. If the Sb and hydrogen effects were additive, one would have expected that the σ_{th} curve would continue to decrease at high Sb concentrations, in the same manner as σ^*. However, the σ_{th} curve flattens-out at around 1250 MPa. Several possible explanations come to mind:

1. At this stress the rate of plastic flow at the notch root may become so slow that surface barriers to hydrogen absorption (*e.g.*, oxide films) form faster than they can be ruptured by plastic flow.
2. Transport of hydrogen in dislocation cores may be the dominant mechanism of hydrogen accumulation ahead of the notch, and this depends on continued plastic flow; therefore, crack formation may not occur when the rate of plastic flow becomes too slow.
3. Neither a surface impedance nor the transport mechanisms may be responsible for the σ_{th} plateau. Rather, it may represent a minimum local stress needed either to nucleate a microcrack at an inclusion (taking account of constraint effects in reducing shear stresses) or to accumulate enough hydrogen at the microcrack tip to enable it to extend to the first grain boundary.

Further research will be required before a choice among these possibilities can be made.

V. SUMMARY

The superimposed effects of intergranular impurity segregation and a gaseous hydrogen environment on the fracture behavior of a Ni-Cr steel have been studied. In the absence of sufficient impurity segregation in this medium-strength (σ_y = 840 MPa) steel, the hydrogen causes Mode II bifurcation of a fatigue precrack at high K levels; this displacement-controlled cracking does not represent brittle behavior in the usual sense. With the segregation of impurities (P, Sn, or Sb) which are known to reduce intergranular cohesion, the threshold K (*i.e.*, K_{th}) for hydrogen-induced extension of the precrack falls to quite low levels; the hydrogen effect is greatest for the weakest embrittling element (P) and for low concentrations of any of the impurities. The value of K_{th} has been shown to represent not the beginning of brittle cracking ahead of the precrack, but rather a later stage at which the resulting reduction in specimen compliance becomes detectable by the displacement transducer. This is the result of the small volume of the highly-stressed region and the steep stress gradient ahead of a precrack.

Experiments on notched specimens in pure bending showed that the local stress for the formation of the first intergranular microcrack, σ_{th}, is a decreasing function of the intergranular impurity concentration and that the impurity effects in hydrogen are in the same order as in air. Except at the highest Sb concentrations, the σ_{th} values were considerably lower than the corresponding microcrack formation stress in air σ^*, especially at low-to-intermediate impurity concentrations. The stress for unstable fracture in H_2 gas was also found to be lower than the σ^* values in air, indicating that fracture in air is initiation-controlled, while in hydrogen it is propagation-controlled.

The results show that, at the yield strength and hydrogen pressure used here, intergranular cracking in hydrogen is primarily an impurity effect. The impurity and hydrogen effects appear to be additive, but some details still need clarification.

The effects of hydrogen cannot be explained on the basis of a static model of hydrogen distribution, because the crack-tip hydrogen concentration would be orders-of-magnitude too low, and hydrogen-induced intergranular cracking is not a static process but a dynamic process. A dynamic model of hydrogen accumulation at the tip of an extending brittle microcrack, outlined here, could account for the observed effects.

ACKNOWLEDGMENTS

This research was supported by the National Science Foundation under grants no. DMR 80-05881 and 78-07535.

REFERENCES

1. D. P. Williams and H. G. Nelson: *Metall. Trans.*, 1970, vol. 1, p. 63.
2. I. M. Bernstein: *Mater. Sci. Eng.*, 1970, vol. 6, p. 1.
3. R. A. Oriani and R. H. Josephic: *Acta Metall.*, 1974, vol. 22, p. 1065.
4. K. Yoshino and C. J. McMahon, Jr.: *Metall. Trans.*, 1974, vol. 5, p. 363.
5. W. W. Gerberich, Y. T. Chen, and C. St. John: *Metall. Trans. A*, 1975, vol. 6A, p. 1485.
6. G. W. Simmon, P. S. Pao, and R. P. Wei: *Metall. Trans. A*, 1978, vol. 9A, p. 1147.
7. S. K. Banerji, C. J. McMahon, Jr., and H. C. Feng: *Metall. Trans. A*, 1978, vol. 9A, p. 233.
8. T. D. Lee, T. Goldenberg, and J. P. Hirth: *Metall. Trans. A*, 1979, vol. 10A, p. 439.
9. N. Bandyopadhyay, J. Kameda, and C. J. McMahon, Jr.: *Metall. Trans. A*, 1983, vol. 14A, p. 881.
10. C. L. Briant, H. C. Feng, and C. J. McMahon, Jr.: *Metall. Trans. A*, 1978, vol. 9A, p. 625.
11. J. Kameda, N. Bandyopadhyay, and C. J. McMahon, Jr.: Proc. of Second JIM Int. Symp., "Hydrogen in Metals", suppl. to *Trans. Japan Inst. Metals*, Minakami, Japan, 1980, vol. 21, p. 437.
12. Y. Takeda and C. J. McMahon, Jr.: *Metall. Trans. A*, 1981, vol. 12A, p. 1255.
13. J. Kameda and C. J. McMahon, Jr.: *Metall. Trans. A*, 1980, vol. 11A, p. 91.
14. J. Kameda and C. J. McMahon, Jr.: *Metall. Trans. A*, 1981, vol. 12A, p. 31.
15. Specification E-399-76, ASTM, Philadelphia, PA, 1976.
16. J. R. Griffiths and D. R. J. Owen: *J. Mech. Phys. Solids*, 1971, vol. 19, p. 419.
17. J. Kameda: *Metall. Trans. A*, 1981, vol. 12A, p. 2039.
18. C. J. McMahon, Jr. and V. Vitek: *Acta Metall.*, 1979, vol. 27, p. 507.
19. M. L. Jokl, V. Vitek, and C. J. McMahon, Jr.: *Acta Metall.*, 1980, vol. 28, p. 1479.
20. H. H. Johnson, J. F. Morlet, and A. R. Troiano: *Trans. TMS-AIME*, 1958, vol. 212, p. 528.
21. A. R. Troiano: *Trans. ASM*, 1960, vol. 52, p. 54.
22. R. A. Oriani: *Ber. Bunsen Besellsch. Phys. Chem.*, 1972, vol. 76, p. 848.
23. C. M. Li, R. A. Oriani, and L. W. Darken: *Z. Phys. Chem.*, 1966, vol. 49, p. 271.
24. J. Kameda and M. L. Jokl: *Scripta Metall.*, 1982, vol. 16, p. 325.
25. C. J. McMahon, Jr., in *Hydrogen Effects in Metals*, I. M. Bernstein and A. W. Thompson, eds., TMS-AIME, 1980, p. 219.